Higgs boson pair production at the LHC: experimental overview

Arnaud Ferrari
Uppsala University, Sweden

UU-HEP seminar, 07/11/2019

Outline

• Introduction

• ATLAS and CMS searches for HH in the $bbbb$, $bb\tau\tau$ and $bb\gamma\gamma$ decay channels with up to 36/fb of 13 TeV pp collision data

• Combination of HH searches in ATLAS and CMS with up to 36/fb of 13 TeV pp collision data

• First HH search results with the full LHC Run-2 dataset

• Prospect studies for HH searches at the HL-LHC (and beyond)

• Conclusion and back-up slides

Introduction

Reminder: the Higgs potential

After discovering the Higgs boson, the ultimate probe of the Standard Model is to fully measure the Higgs potential.

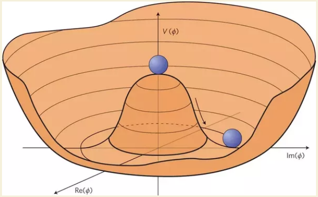

$$V(\Phi) = -\frac{1}{2}\mu^2\Phi^2 + \frac{1}{4}\lambda\Phi^4 \overset{\Phi\to v+H}{=} \lambda v^2 H^2 + \lambda v H^3 + \frac{1}{4}\lambda H^4$$

mass term: $\frac{1}{2}m_H^2 H^2$

self-interaction terms

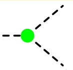

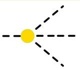

$\rightarrow v = \mu/\sqrt{\lambda} = 246$ GeV and $\lambda = m_H^2/(2v^2) = 0.13$ fully determine the shape of the Higgs potential.

$\Longrightarrow$ *In order to further test the Standard Model, one must observe $H \to HH$!*

SM Higgs boson pair production

Gluon-gluon fusion:

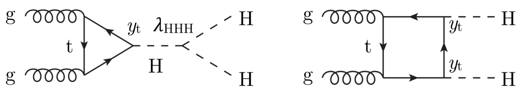

Due to the destructive interference between the Higgs boson self-coupling and box diagrams, the SM cross-section for Higgs boson pair production is very small, i.e. about three orders of magnitude less than for single Higgs boson production.

$\sqrt{s}$	7 TeV	8 TeV	13 TeV	14 TeV	27 TeV	100 TeV
$\sigma_{NNLO\ FTapprox}$ [fb]	6.572	9.441	31.05	36.69	139.9	1224
Scale unc.	$-6.5\%^{+3.0\%}$	$-6.1\%^{+2.8\%}$	$-5.0\%^{+2.2\%}$	$-4.9\%^{+2.1\%}$	$-3.9\%^{+1.3\%}$	$-3.2\%^{+0.9\%}$
PDF unc.	±3.5%	±3.1%	±2.1%	±2.1%	±1.7%	±1.7%
αS unc.	±2.6%	±2.4%	±2.1%	±2.1%	±1.8%	±1.7%
PDF+αS unc.	±4.3%	±3.9%	±3.0%	±3.0%	±2.5%	±2.4%
mtop unc.	±2.2%	±2.3%	±2.6%	±2.7%	±3.4%	±4.6%

From https://twiki.cern.ch/twiki/bin/view/LHCPhysics/LHCHXSWGHH

Other production modes: even smaller cross-sections...

BSM Higgs boson pair production

Enhancements of the HH production cross-section and modified kinematics (e.g. m_{HH}, $p_T^{H(H)}$) could occur through variations of the top-Yukawa- and/or Higgs-self-couplings, as well as new vertices (e.g. in Effective Field Theories).

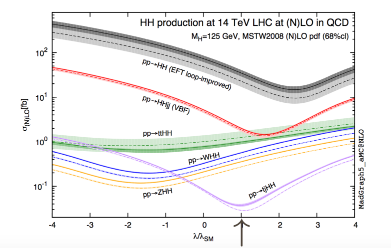

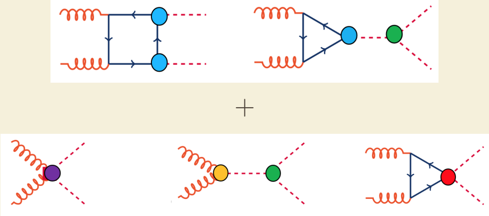

Resonant Higgs boson pair production:

- Randall-Sundrum graviton (spin-2): $G \to HH$
- 2HDM heavy Higgs boson (spin-0): $X \to HH$

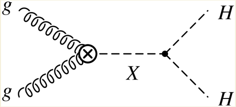

Overview of HH search channels

	bb	WW	ττ	ZZ	γγ
bb	33%				
WW	25%	4.6%			
ττ	7.4%	2.5%	0.39%		
ZZ	3.1%	1.2%	0.34%	0.076%	
γγ	0.26%	0.10%	0.029%	0.013%	0.0053%

Many final states to explore... The main focus of this talk is the *non-resonant* HH production mode and reviews of:

- $bbbb$, $bb\gamma\gamma$ and $bb\tau\tau$ with 36/fb of data;
- statistical combinations with 36/fb of data;
- new results with the full Run-2 dataset;
- prospect studies.

See back-up for results on resonant HH...

Run-1 legacy – ATLAS:

Analysis	$\gamma\gamma bb$	$\gamma\gamma WW^*$	$bb\tau\tau$	$bbbb$	Combined
		Upper limit on the cross section [pb]			
Expected	1.0	6.7	1.3	0.62	0.47
Observed	2.2	11	1.6	0.62	0.69
		Upper limit on the cross section relative to the SM prediction			
Expected	100	680	130	63	48
Observed	220	1150	160	63	70

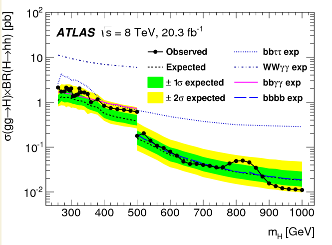

Phys. Rev. D 92, 092004 (2015)

Overview of HH search channels

	bb	WW	ττ	ZZ	γγ
bb	33%				
WW	25%	4.6%			
ττ	7.4%	2.5%	0.39%		
ZZ	3.1%	1.2%	0.34%	0.076%	
γγ	0.26%	0.10%	0.029%	0.013%	0.0053%

Many final states to explore... The main focus of this talk is the *non-resonant* HH production mode and reviews of:

- $bbbb$, $bb\gamma\gamma$ and $bb\tau\tau$ with 36/fb of data;
- statistical combinations with 36/fb of data;
- new results with the full Run-2 dataset;
- prospect studies.

See back-up for results on resonant HH...

Run-1 legacy – CMS:

- $bbbb + bb\gamma\gamma + bb\tau\tau$
- Expected: $0.47^{+0.20}_{-0.12}$ pb ($47 \times$ SM)
- Observed: 0.43 pb ($43 \times$ SM)

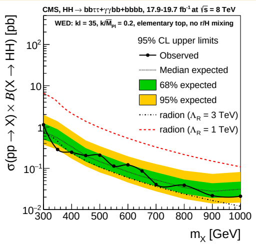

Phys. Rev. D 96, 072004 (2016)

ATLAS and CMS searches for HH in the $bbbb$, $bb\tau\tau$ and $bb\gamma\gamma$ decay channels with up to 36/fb of 13 TeV pp collision data

$HH \to bbbb$ – event topologies

- **ATLAS → one paper [JHEP01 (2019) 030] with two event topologies:**
  - Non-resonant $HH \to bbbb$ + "light" HH resonances: resolved topology.
  - Resonant production of $HH \to bbbb$ with mass $\gtrsim$1 TeV: boosted topology.

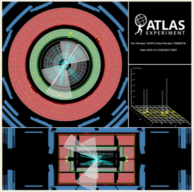

Topology/ Objects	Resolved (260-1400 GeV)	Boosted (800-3000 GeV)
Triggers and corresponding $\int Ldt$ (fb^{-1})	Combination of b-jet triggers 3.2+24.3	Single large-R jet trigger 36.1
N_{jets} p_T cut	$\geq$4 jets, $R = 0.4$ 40 GeV	$\geq$2 jets, $R = 1.0$ 450 / 250 GeV
b-tagging $N_{\text{b-jets}}$	70% for all jets 4	70% on track-jets with $R = 0.2$ $2, 3, 4$

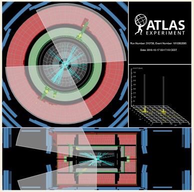

- **CMS → four papers with distinct event topologies:**
  - Non-resonant HH: 35.9/fb; $\geq$4 jets ($R = 0.4$) with p_T above 30 GeV; 4 b-tags (resolved topology) in JHEP04 (2019) 112.
  - Resonant HH with a resolved topology in JHEP08 (2018) 052.
  - Resonant HH with two jets of $R = 0.8$ in Phys. Lett. B 781 (2018) 244, or using semi-resolved events in JHEP01 (2019) 040.

ATLAS non-resonant $HH \to bbbb$

Event selection:

- Selection and pairing of the 4 jets with highest b-tagging into H candidates using ΔR_{jj}, m_{4j} and differences in m_{2j}.
- m_{4j}- and m_{2j}-dependent requirements on the p_T and mass of the H candidates $\Rightarrow$ SR around $(120\ \text{GeV}; 110\ \text{GeV})$.
- Events in which a 3-jet combination is compatible with a top-quark decay are vetoed.

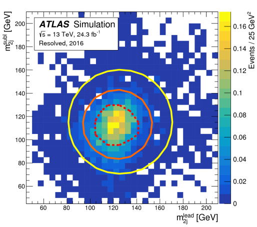

Background estimation:

- Multi-jet: weights are derived by comparing $2b{+}2j$ and $4b$ samples in a sideband (SB), then applied to a $2b{+}2j$ sample of the SR (one H from 2 b-jets, one H from 2 non-b-jets).
- $t\bar{t}$: simulated m_{4j} shapes (hadronic and semi-leptonic).
- Normalisation: simultaneous fit of 3 background-enriched regions of the SB.
- Validation: m_{4j} in a control region between SR and SB.

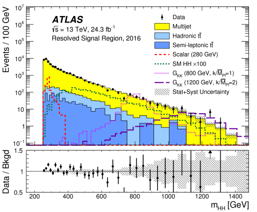

Results:

Simultaneous fit of m_{4j} in the 2015 and 2016 dataset $\Rightarrow$ 95% CL upper limits in units of σ^{HH}_{SM}:

Observed	-2σ	-1σ	Expected	$+1\sigma$	$+2\sigma$
13.0	11.1	14.9	20.7	30.0	43.5

CMS non-resonant $HH \to bbbb$

Event selection:

- Triggers: OR two paths of at least 4 jets with 3 b-tags.
- Selection and pairing of the 4 jets with highest b-tagging into H candidates using differences in m_{2j}.
- BDT classifier to separate HH from the background.

HH system	H candidates	Jet variables
M_X, M_{HH},	M_{H_1}, M_{H_2}	$p_{T_j}^{(i=1-4)}$, $\eta_j^{(i=1-4)}$,
$p_T^{H_1H_2}$	$p_T^{H_1}$, $p_T^{H_2}$	H_T^{rest}, H_T
$\cos\theta^*_{H_1H_2-H_1}$	$\cos\theta^*_{H_1-j_1}$	$CMVA_3$, $CMVA_4$
	$\Delta R_{jj}^{H_1}$, $\Delta R_{jj}^{H_2}$, $\Delta\phi_{jj}^{H_1}$, $\Delta\phi_{jj}^{H_2}$	

Background modelling via hemisphere mixing:

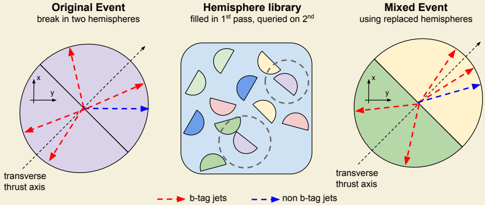

- transverse thrust axis $\to$ where the sum of the absolute values of the projections of the p_T of the jets is maximal;
- two hemispheres are only mixed if similar enough to original hemispheres;
- the method destroys any correlation between two hemispheres, ensuring no signal contamination;
- three new samples for: (i) BDT training, (ii) validation purposes, (iii) prediction of the optimized BDT shape.

CMS non-resonant $HH \to bbbb$

Event selection:

- Triggers: OR two paths of at least 4 jets with 3 b-tags.
- Selection and pairing of the 4 jets with highest b-tagging into H candidates using differences in m_{2j}.
- BDT classifier to separate HH from the background.

HH system	H candidates	Jet variables
M_X, M_{HH},	M_{H_1}, M_{H_2}	$p_{T_j}^{(i=1-4)}$, $\eta_j^{(i=1-4)}$,
$p_T^{H_1 H_2}$	$p_T^{H_1}$, $p_T^{H_2}$	H_T^{rest}, H_T
$\cos\theta^*_{H_1 H_2 - H_1}$	$\cos\theta^*_{H_1 - j_1}$	$CMVA_3$, $CMVA_4$
	$\Delta R_{jj}^{H_1}$, $\Delta R_{jj}^{H_2}$, $\Delta\phi_{jj}^{H_1}$, $\Delta\phi_{jj}^{H_2}$	

Background modelling via hemisphere mixing:

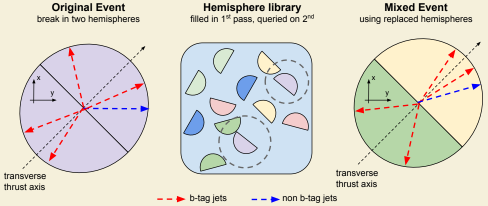

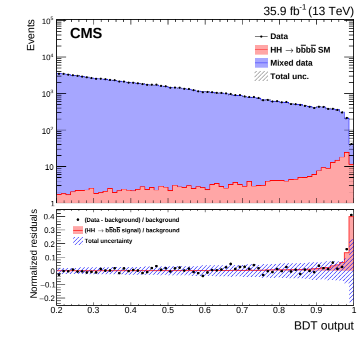

95% CL upper limits in units of σ_{SM}^{HH}:

Observed	-2σ	-1σ	Expected	$+1\sigma$	$+2\sigma$
74.6	19.4	26.1	36.9	52.9	73.4

ATLAS non-resonant $HH \to bb\gamma\gamma$

Event selection:

- 2 photons (trigger and offline), $E_T/m_{\gamma\gamma} > 0.35 / 0.25$ & $m_{\gamma\gamma} \subset [105; 160]$ GeV.
- At least 2 central jets with $p_T > 25$ GeV:
  - 2-tag: exactly 2 b-jets (70%),
  - 1-tag: fails 2-tag but has 1 b-jet (60%) + BDT to choose the second jet.
- Leading jet $p_T > 100$ GeV, sub-leading jet $p_T > 30$ GeV & $m_{jj} \subset [90; 140]$ GeV.

The analysis strategy is to fit the $m_{\gamma\gamma}$ distribution

- Signal & single-H background: simulation, double-sided Crystal Ball function.
- Continuum background: fit to the data with a first-order exponential to minimise the spurious signal (bias from fitting a signal+background model to a background-only sample).

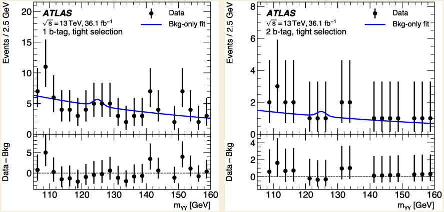

95% CL upper limits on $\sigma_{gg\to HH}$:

	Observed	Expected	-1σ	$+1\sigma$
$\sigma_{gg\to HH}$ [pb]	0.73	0.93	0.66	1.4
As a multiple of σ_{SM}	22	28	20	40

[JHEP11 (2018) 040]

CMS non-resonant $HH \to bb\gamma\gamma$

Event selection and categorisation:

- 2 photons (trigger and offline), $E_T/m_{\gamma\gamma} > 0.33\,/\,0.25$ & $m_{\gamma\gamma} \subset [100;180]$ GeV.
- 2 b-tagged central jets with $p_T > 25$ GeV & $m_{jj} \subset [70;190]$ GeV after b-jet energy regression.
- Low/high-mass regions if $\tilde{M}_X = m_{\gamma\gamma jj} - (m_{\gamma\gamma} - m_H) - (m_{jj} - m_H)$ is below/above 350 GeV.
- In each category: BDT using b-tagging, helicity and HH transverse balance input variables $\to$ categorisation into high/medium-purity regions based on the BDT score.

Statistical analysis: 2D fit per category

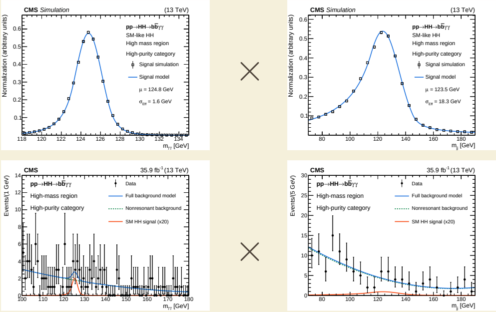

- Signal (including VBF HH events): double-sided Crystal-Ball function.
- Backgrounds ($n\gamma$+jets and single-H): Bernstein polynomial or double-sided Crystal-Ball function.
- Unbinned maximum-likelihood to the 2D $m_{\gamma\gamma} - m_{jj}$ distribution.

$\to$ 95% CL upper limits in units of σ_{SM}^{HH}:

Observed	-1σ	Expected	$+1\sigma$
24	13	19	30

[Phys. Lett. B 788 (2019) 7]

ATLAS non-resonant $HH \to bb\tau\tau$

2 sub-channels ($\tau_\ell\tau_h$ & $\tau_h\tau_h$) but 3 signal regions based on the trigger:

- $\tau_\ell\tau_h$ channel:
  - Single-lepton trigger (SLT)
  - If !SLT, lepton+τ trigger (LTT)
- $\tau_h\tau_h$ channel:
  - Single- (STT) or di-τ (DTT) trigger

- ℓ+τ_h or 2-τ_h opposite-sign systems;
- Trigger-dependent cuts on (p_T^ℓ; $p_T^{\tau_h}$) or $p_T^{\tau_{1(2)}}$;
- $\geq$2 jets, $p_T^{j_{1(2)}} > 45$-80 (20) GeV;
- 2 b-jets and $m_{\tau\tau}^{\text{MMC}} > 60$ GeV.

BDTs are used to separate the signal from the following backgrounds:

- Top-quark backgrounds with true τ_h: simulation + normalisation from data at low BDT;
- $Z \to \tau\tau + bb/bc/cc$: simulation + normalisation from a single-bin $Z \to \mu\mu + bb$ region in data;
- Jet $\to$ fake τ_h: (semi-)data-driven methods... and all other backgrounds from simulation.

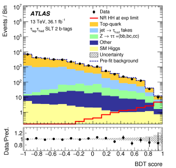

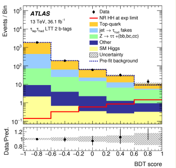

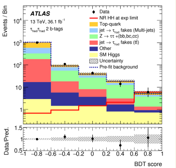

		Observed	-1σ	Expected	$+1\sigma$
$\tau_{\text{lep}}\tau_{\text{had}}$	$\sigma(HH \to bb\tau\tau)$ [fb]	57	49.9	69	96
	$\sigma/\sigma_{\text{SM}}$	23.5	20.5	28.4	39.5
$\tau_{\text{had}}\tau_{\text{had}}$	$\sigma(HH \to bb\tau\tau)$ [fb]	40.0	30.6	42.4	59
	$\sigma/\sigma_{\text{SM}}$	16.4	12.5	17.4	24.2
Combination	$\sigma(HH \to bb\tau\tau)$ [fb]	30.9	26.0	36.1	50
	$\sigma/\sigma_{\text{SM}}$	12.7	10.7	14.8	20.6

Most stringent limits at the LHC:
obs. (exp.): $12.7\,(14.8) \times \sigma_{SM}^{HH}$

[Phys. Rev. Lett. 121, 191801]

CMS non-resonant $HH \to bb\tau\tau$

Event selection:

- Three sub-channels ($\tau_e\tau_h$, $\tau_\mu\tau_h$ & $\tau_h\tau_h$), with neither LTT nor STT trigger;
- $p_T(e/\mu) > 27/23$ GeV; $p_T(\tau_h) > 20$ GeV $[\tau_\ell\tau_h]$ or 45 GeV $[\tau_h\tau_h]$; $p_T(j_{1,2}) > 20$ GeV;
- Two SR categories (≥2b and 1b1j), where the two jets can be resolved or merged;
- Elliptic cut in the $(m_{\tau\tau}; m_{bb})$ plane, where $H \to \tau\tau$ is reconstructed with SVfit;
- $\tau_\ell\tau_h$: cut on a BDT score to reduce $t\bar{t}$, fit the stransverse mass m_{T2};
- $\tau_h\tau_h$: fit m_{T2}.

Backgrounds:

- $Z \to \tau\tau + bb/bc/cc$: simulation + data-driven correction of the jet emission model;
- Multi-jet from SS data (yield correction using OS/SS events with inverted τ isolation);
- All other backgrounds from simulation.

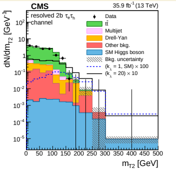

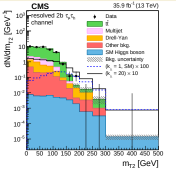

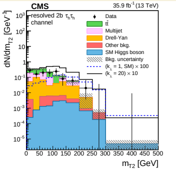

95% CL upper limits in units of $\sigma^{HH}_{\rm SM}$:

Observed	-1σ	Expected	$+1\sigma$
31	17	25	37

[Phys. Lett. B 778 (2018) 101]

Combination of HH searches in ATLAS and CMS with up to 36/fb of 13 TeV pp collision data

CMS – non-resonant HH – combination

Combination of the 3 most sensitive channels ($bb\gamma\gamma$, $bb\tau\tau$ and $bbbb$) with a sub-leading di-lepton $bbVV$ channel:

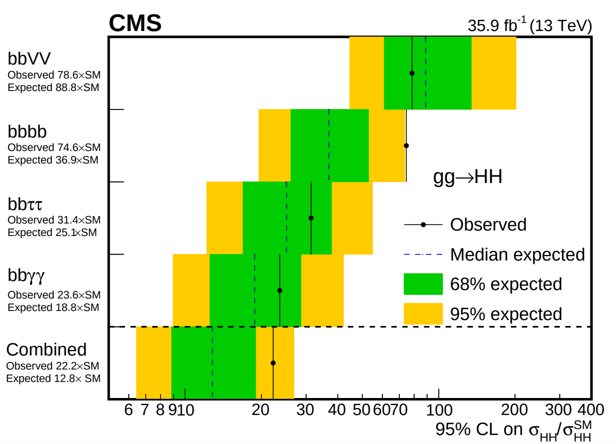

JHEP01 (2018) 054

JHEP04 (2019) 112

Phys. Lett. B 778 (2018) 101

Phys. Lett. B 788 (2019) 7

Phys. Rev. Lett. 122 (2019) 121803

CMS considers new couplings derived from dimension-6 operators (EFT):

$$\mathcal{L}_{\mathrm{HH}} = \boxed{\kappa_\lambda}\lambda^{\mathrm{SM}}_{\mathrm{HHH}} v\, H^3 - \frac{m_{\mathrm{t}}}{v}\left(\boxed{\kappa_{\mathrm{t}}}H + \frac{\boxed{c_2}}{v}H^2\right)\left(\bar{\mathrm{t}}_{\mathrm{L}}\mathrm{t}_{\mathrm{R}} + \mathrm{h.c.}\right) + \frac{1}{4}\frac{\alpha_S}{3\pi v}\left(\boxed{c_{\mathrm{g}}}H - \frac{\boxed{c_{2\mathrm{g}}}}{2v}H^2\right)G^{\mu\nu}G_{\mu\nu}$$

EFT couplings yield different m_{HH} and $\cos\theta^*_H$ distributions, but they can be clustered into 12 typical shape benchmarks after a full scan.

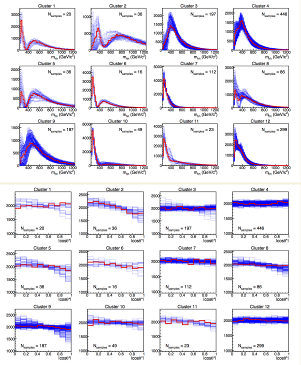

CMS has published limits on non-resonant HH for every shape benchmark:

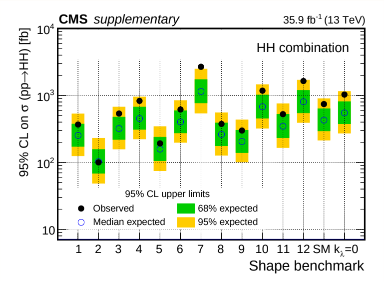

CMS – non-resonant HH – EFTs (1)

CMS considers new couplings derived from dimension-6 operators in SMEFT:

$$\mathcal{L}_{\mathrm{HH}} = \boxed{\kappa_\lambda} \lambda^{\mathrm{SM}}_{\mathrm{HHH}} v H^3 - \frac{m_t}{v}\left(\boxed{\kappa_t} H + \frac{\boxed{c_2}}{v} H^2\right)\left(\bar{t}_L t_R + \mathrm{h.c.}\right) + \frac{1}{4}\frac{\alpha_S}{3\pi v}\left(\boxed{c_g} H - \frac{\boxed{c_{2g}}}{2v} H^2\right) G^{\mu\nu} G_{\mu\nu}$$

EFT couplings yield different m_{HH} and $\cos\theta^*_H$ distributions, but they can be clustered into 12 typical shape benchmarks after a full scan.

Benchmark	κ_λ	κ_t	c_2	c_g	c_{2g}
1	7.5	1.0	−1.0	0.0	0.0
2	1.0	1.0	0.5	−0.8	0.6
3	1.0	1.0	−1.5	0.0	−0.8
4	−3.5	1.5	−3.0	0.0	0.0
5	1.0	1.0	0.0	0.8	−1
6	2.4	1.0	0.0	0.2	−0.2
7	5.0	1.0	0.0	0.2	−0.2
8	15.0	1.0	0.0	−1	1
9	1.0	1.0	1.0	−0.6	0.6
10	10.0	1.5	−1.0	0.0	0.0
11	2.4	1.0	0.0	1	−1
12	15.0	1.0	1.0	0.0	0.0
SM	1.0	1.0	0.0	0.0	0.0

CMS has published limits on non-resonant HH for every shape benchmark:

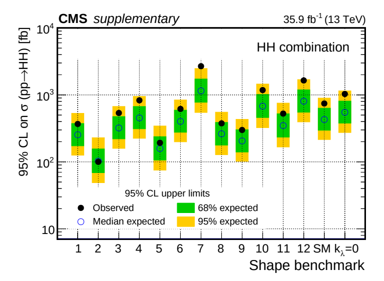

CMS – non-resonant HH – EFTs (2)

At LO, $\sigma(gg \to HH)$ can be expressed as a function of the EFT couplings.

$$R_{hh} \equiv \frac{\sigma_{hh}}{\sigma_{hh}^{SM}} = \mathrm{Poly}(\mathbf{A}) = A_1\,\kappa_t^4 + A_2\,c_2^2 + (A_3\,\kappa_t^2 + A_4\,c_g^2)\,\kappa_\lambda^2 + A_5\,c_{2g}^2 + (A_6\,c_2 + A_7\,\kappa_t\kappa_\lambda)\kappa_t^2 + (A_8\,\kappa_t\kappa_\lambda + A_9\,c_g\kappa_\lambda)c_2 + A_{10}\,c_2c_{2g} + (A_{11}\,c_g\kappa_\lambda + A_{12}\,c_{2g})\,\kappa_t^2 + (A_{13}\,\kappa_\lambda c_g + A_{14}\,c_{2g})\,\kappa_t\kappa_\lambda + A_{15}\,c_gc_{2g}\kappa_\lambda$$

- Can also be applied to differential cross-sections $\Rightarrow R^j_{HH} = \mathrm{Poly}(\mathbf{A}^j)$ [arxiv:1710.08261].
- Emulate any EFT parameters via reweighting based on true m^i_{HH} and $\cos\theta^*_i$ at LO from an ensemble of shape benchmarks.

$$W_i = \frac{R_{hh}(m^i_{HH}, \cos\theta^*_i)}{N_i} \cdot \frac{\sigma^{\mathrm{SM}}_{hh}\,\mathrm{Frac}^j_{\mathrm{SM}}}{\sigma_{hh}\,C_{\mathrm{norm}}}$$

$$C_{\mathrm{norm}} = \sum_j R^j_{hh}\frac{\sigma^{\mathrm{SM}}_{hh}}{\sigma_{hh}}\mathrm{Frac}^j_{\mathrm{SM}}$$

Setting all other EFT couplings to their SM value, a scan of the Higgs boson self-coupling leads to observed (expected) κ_λ-values to be constrained @ 95% CL to:

$$-11.8 < \kappa_\lambda < 18.8\ (-7.1 < \kappa_\lambda < 13.6)$$

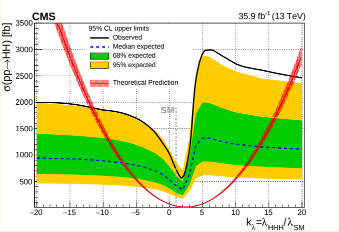

ATLAS – non-resonant HH – combination

Combination of the 3 most sensitive channels ($bb\tau\tau$, $bbbb$ and $bb\gamma\gamma$) with 3 sub-leading channels (multi-lepton $WWWW$, single-lepton $WW\gamma\gamma$ and single-lepton $bbWW$):

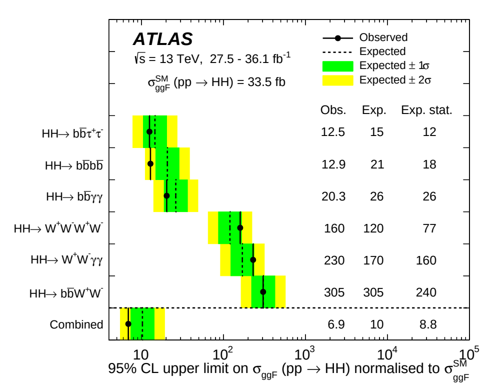

Phys. Rev. Lett. 121, 191801

JHEP01 (2019) 030

JHEP11 (2018) 040

JHEP05 (2019) 124

Eur. Phys. J. C 78 (2018) 1007

JHEP04 (2019) 092

---

https://arxiv.org/abs/1906.02025

ATLAS – non-resonant HH – variation of the Higgs boson self-coupling

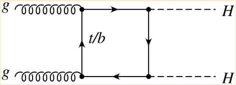

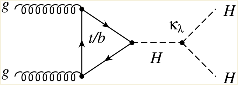

Variations of κ_λ affect the interference, hence m_{HH} and the signal acceptances.

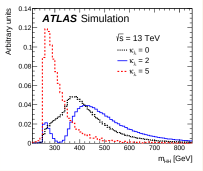

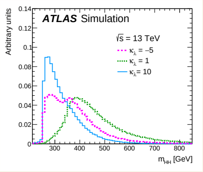

Currently, the LO mode of MG5_aMC@NLO is used, in which BSM couplings are switched-off, with varied κ_λ values. A linear combination of 3 samples is performed, followed by a m_{HH} reweighting of the NLO SM sample.

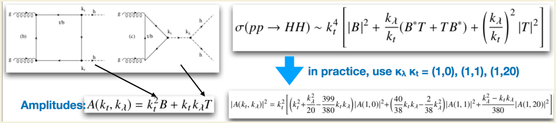

A dedicated NLO POWHEG package with varied κ_λ is available for the end-of-Run-2 analyses.

ATLAS – non-resonant HH – variation of the Higgs boson self-coupling

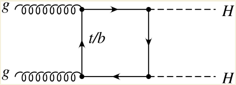

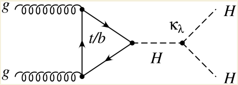

Variations of κ_λ affect the interference, hence m_{HH} and the signal acceptances.

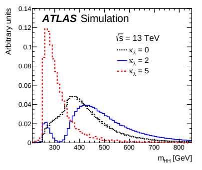

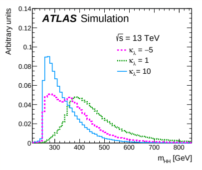

With $\kappa_t = 1$, the Higgs boson self-coupling is observed (expected) to be constrained @ 95% CL to:

$$-5.0 < \kappa_\lambda < 12.0 \; (-5.8 < \kappa_\lambda < 12.0)$$

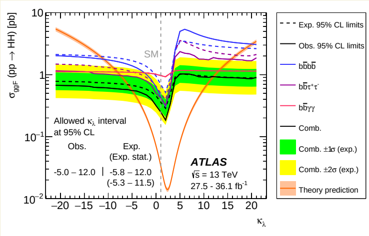

ATLAS – non-resonant HH... combined with single-Higgs-boson measurements

κ_λ also has an impact on single-Higgs-boson production and decays at electroweak NLO!

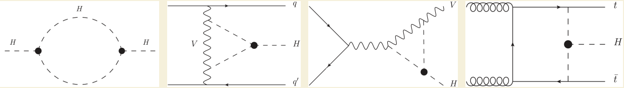

Using the framework of Eur. Phys. J. C 77 (2017) 887, global fit of κ_λ based on combined single-Higgs-boson measurements (including event kinematic information) in 36–80/fb of data: ATL-PHYS-PUB-2019-009.

- Observed (expected) 95% CL interval constraint: $-3.2 < \kappa_\lambda < 11.9$ ($-6.2 < \kappa_\lambda < 14.4$).
- Negative log-likelihood contours either in $(\kappa_\lambda, \kappa_F)$ with $\kappa_V = 1$ or in $(\kappa_\lambda, \kappa_V)$ with $\kappa_F = 1$.

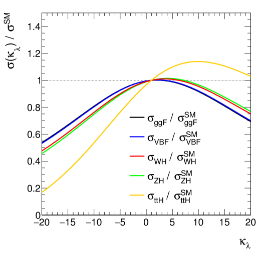

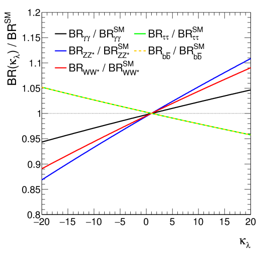

ATLAS – non-resonant HH... combined with single-Higgs-boson measurements

κ_λ also has an impact on single-Higgs-boson production and decays at electroweak NLO!

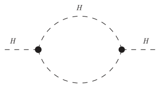

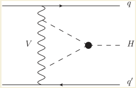

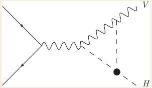

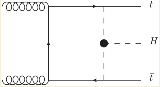

Using the framework of Eur. Phys. J. C 77 (2017) 887, global fit of κ_λ based on combined single-Higgs-boson measurements (including event kinematic information) in 36–80/fb of data: ATL-PHYS-PUB-2019-009.

- Observed (expected) 95% CL interval constraint: $-3.2 < \kappa_\lambda < 11.9$ ($-6.2 < \kappa_\lambda < 14.4$).
- Negative log-likelihood contours either in $(\kappa_\lambda, \kappa_F)$ with $\kappa_V = 1$ or in $(\kappa_\lambda, \kappa_V)$ with $\kappa_F = 1$.

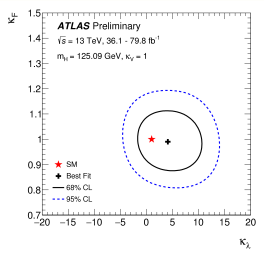

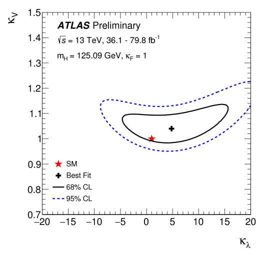

ATLAS – non-resonant HH... combined with single-Higgs-boson measurements

Next: combine the single- and double-Higgs-boson measurements/searches: ATLAS-CONF-2019-049.

Analysis	Integrated luminosity (fb^{-1})	Ref.
$H \to \gamma\gamma$ (excluding $t\bar{t}H$, $H \to \gamma\gamma$)	79.8	[21,22]
$H \to ZZ^* \to 4\ell$ (including $t\bar{t}H$, $H \to ZZ^* \to 4\ell$)	79.8	[23,24]
$H \to WW^* \to e\nu\mu\nu$	36.1	[25]
$H \to \tau^+\tau^-$	36.1	[26]
VH, $H \to b\bar{b}$	79.8	[27,28]
$t\bar{t}H$, $H \to b\bar{b}$	36.1	[29]
$t\bar{t}H$, $H \to$ multilepton	36.1	[30]
$HH \to b\bar{b}b\bar{b}$	27.5	[31]
$HH \to b\bar{b}\tau^+\tau^-$	36.1	[32]
$HH \to b\bar{b}\gamma\gamma$	36.1	[33]

- Observed (expected) 95% CL interval constraint: $-2.3 < \kappa_\lambda < 10.3$ ($-5.1 < \kappa_\lambda < 11.2$).
- Likelihood fit with other couplings set to SM values:

$$\kappa_\lambda = 4.6^{+2.9}_{-3.5}(\text{stat.})^{+1.2}_{-1.2}(\text{exp.})^{+0.7}_{-0.5}(\text{sig. th.})^{+0.6}_{-1.0}(\text{bkg. th.})$$

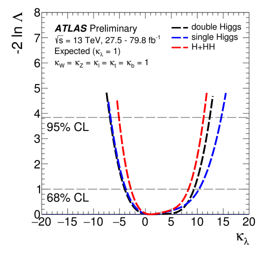

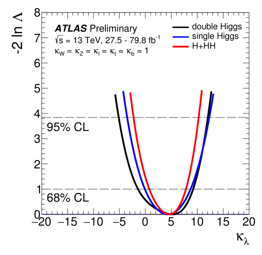

ATLAS – non-resonant HH... combined with single-Higgs-boson measurements

- Generic model: κ_W, κ_Z, κ_t, κ_b, κ_ℓ and κ_λ are fitted simultaneously.

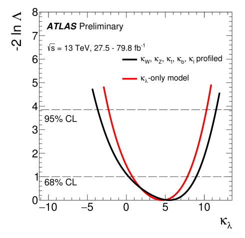

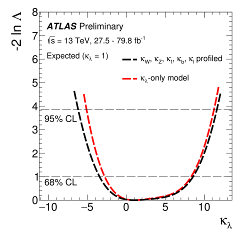

Model	$\kappa_W{}^{+1\sigma}_{-1\sigma}$	$\kappa_Z{}^{+1\sigma}_{-1\sigma}$	$\kappa_t{}^{+1\sigma}_{-1\sigma}$	$\kappa_b{}^{+1\sigma}_{-1\sigma}$	$\kappa_\ell{}^{+1\sigma}_{-1\sigma}$	$\kappa_\lambda{}^{+1\sigma}_{-1\sigma}$	κ_λ [95% CL]	
κ_λ-only	1	1	1	1	1	$4.6^{+3.2}_{-3.8}$	$[-2.3, 10.3]$	obs.
						$1.0^{+7.3}_{-3.8}$	$[-5.1, 11.2]$	exp.
Generic	$1.03^{+0.08}_{-0.08}$	$1.10^{+0.09}_{-0.09}$	$1.00^{+0.12}_{-0.11}$	$1.03^{+0.20}_{-0.18}$	$1.06^{+0.16}_{-0.16}$	$5.5^{+3.5}_{-5.2}$	$[-3.7, 11.5]$	obs.
	$1.00^{+0.08}_{-0.08}$	$1.00^{+0.08}_{-0.08}$	$1.00^{+0.12}_{-0.12}$	$1.00^{+0.21}_{-0.19}$	$1.00^{+0.16}_{-0.15}$	$1.0^{+7.6}_{-4.5}$	$[-6.2, 11.6]$	exp.

First HH search results with the full LHC Run-2 dataset

ATLAS – non-resonant $HH \to bb\ell\ell\nu\nu$

New ATLAS non-resonant HH search result based on the full Run-2 dataset (139/fb): https://arxiv.org/abs/1908.06765

Event selection and analysis strategy:

- Signal = $H \to bb$ + $H \to \ell\ell\nu\nu$ (via WW^*, ZZ^* or $\tau\tau$).
- Single- or di-lepton trigger; 2 OS electrons and/or muons & ≥ 2 b-jets; $m_{\ell\ell} \subset [20; 60]$ GeV & $m_{b_1 b_2} \subset [110; 140]$ GeV;
- Define regions with same- or different-flavour (SF vs DF) leptons;
- Main backgrounds after the event pre-selection:
  - di-lepton $t\bar{t}$ & Wt = Top;
  - $Z/\gamma^* \to ee, \mu\mu$ + jets = $Z\ell\ell$;
  - $Z/\gamma^* \to \tau\tau$ + jets = $Z\tau\tau$.

$\Rightarrow$ DNN classifier to distinguish $HH \to bbWW^* \to bb\ell\nu\ell\nu$ from the 3 main backgrounds.

(p_T, η, ϕ)	p_T, η, and ϕ of the leptons, leading two signal jets, and leading two b-tagged jets
Dilepton flavour	Whether the event is composed of two electrons, two muons, or one of each
$\Delta R_{\ell\ell}$, $\lvert\Delta\phi_{\ell\ell}\rvert$	ΔR and magnitude of the $\Delta\phi$ between the two leptons
$m_{\ell\ell}$, $p_T^{\ell\ell}$	Invariant mass and the transverse momentum of the dilepton system
E_T^{miss}, E_T^{miss}-ϕ	Magnitude of the missing transverse momentum vector and its ϕ component
$\lvert\Delta\phi(\mathbf{p}_T^{miss}, \mathbf{p}_T^{\ell\ell})\rvert$	Magnitude of the $\Delta\phi$ between the $\mathbf{p}_T^{miss}$ and the transverse momentum of the dilepton system
$\lvert\mathbf{p}_T^{miss} + \mathbf{p}_T^{\ell\ell}\rvert$	Magnitude of the vector sum of the $\mathbf{p}_T^{miss}$ and the transverse momentum of the dilepton system
Jet multiplicities	Numbers of b-tagged and non-b-tagged jets
$\lvert\Delta\phi_{bb}\rvert$	Magnitude of the $\Delta\phi$ between the leading two b-tagged jets
m_{T2}^{bb}	m_{T2} using the leading two b-tagged jets as the visible inputs and $\mathbf{p}_T^{miss}$ as invisible input
H_{T2}	Scalar sum of the magnitudes of the momenta of the $H \to \ell\nu\ell\nu$ and $H \to bb$ systems, $H_{T2} = \lvert\mathbf{p}_T^{miss} + \mathbf{p}_T^{\ell,0} + \mathbf{p}_T^{\ell,1}\rvert + \lvert\mathbf{p}_T^{b,0} + \mathbf{p}_T^{b,1}\rvert$
H_{T2}^{R}	Ratio of H_{T2} and scalar sum of the transverse momenta of the H decay products, $H_{T2}^{R} = H_{T2}/(E_T^{miss} + \lvert\mathbf{p}_T^{\ell,0}\rvert + \lvert\mathbf{p}_T^{\ell,1}\rvert + \lvert\mathbf{p}_T^{b,0}\rvert + \lvert\mathbf{p}_T^{b,1}\rvert)$, where $\mathbf{p}_T^{\ell(b),0\{1\}}$ are the transverse momenta of the leading {subleading} lepton (b-tagged jet)

ATLAS – non-resonant $HH \to bb\ell\ell\nu\nu$

New ATLAS non-resonant HH search result based on the full Run-2 dataset (139/fb): https://arxiv.org/abs/1908.06765

Event selection and analysis strategy:

- Signal = $H \to bb$ + $H \to \ell\ell\nu\nu$ (via WW^*, ZZ^* or $\tau\tau$).
- Single- or di-lepton trigger; 2 OS electrons and/or muons & $\geq$2 b-jets; $m_{\ell\ell} \subset [20; 60]$ GeV & $m_{b_1 b_2} \subset [110; 140]$ GeV;
- Define regions with same- or different-flavour (SF vs DF) leptons;
- Main backgrounds after the event pre-selection:
  - di-lepton $t\bar{t}$ & Wt = Top;
  - $Z/\gamma^* \to ee, \mu\mu$ + jets = $Z\ell\ell$;
  - $Z/\gamma^* \to \tau\tau$ + jets = $Z\tau\tau$.

$\Rightarrow$ DNN classifier to distinguish $HH \to bbWW^* \to b b\ell\nu\ell\nu$ from the 3 main backgrounds.

$\Rightarrow$ 4 outputs p_i (with $\sum p_i = 1$), $i \subset \{HH, \text{Top}, Z\ell\ell, Z\tau\tau\}$.

p_{HH} | p_{Top} | $p_{Z\ell\ell}$ | $p_{Z\tau\tau}$

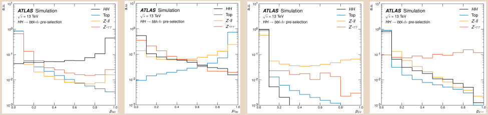

ATLAS – non-resonant $HH \to bb\ell\ell\nu\nu$

Besides $m_{\ell\ell}$ and m_{bb}, another discriminant in the analysis is: $d_{HH} = \ln\left(\frac{p_{HH}}{p_{\text{Top}} + p_{Z\ell\ell} + p_{Z\tau\tau}}\right)$.

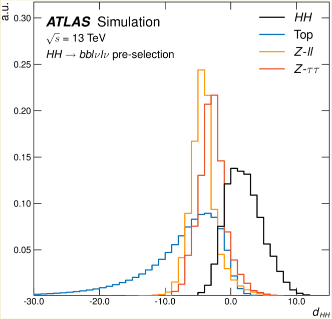

- Two signal regions: SR-SF with $d_{HH} > 5.45$ & SR-DF with $d_{HH} > 5.55$;
- Two control regions: CR-Top and CR-Z+HF to normalise the corresponding backgrounds;
- Two signal-depleted validation regions to check the normalisation of the backgrounds.

ATLAS – non-resonant $HH \to bb\ell\ell\nu\nu$

Besides $m_{\ell\ell}$ and m_{bb}, another discriminant in the analysis is: $d_{HH} = \ln\left(\frac{p_{HH}}{p_{\text{Top}} + p_{Z\ell\ell} + p_{Z\tau\tau}}\right)$.

Region Definitions						
Observable	**CR-Top**	**VR-1**	**CR-Z+HF**	**VR-2**	**SR-SF**	**SR-DF**
Dilepton Flavour	DF	SF	DF or SF	SF	SF	DF
$m_{\ell\ell}$ [GeV]	(20, 60)	(20, 60)	(81.2, 101.2)	(71.2, 81.2) or (101.2, 115)	(20, 60)	(20, 60)
m_{bb} [GeV]	$\notin$ (100, 140)	> 140	(100, 140)	(100, 140)	(110, 140)	(110, 140)
d_{HH}	> 4.5	> 4.5	> 0	> 0	> 5.45	> 5.55
Event Yields						
Data	108	171	852	157	16	9
Total Bkg.	108 ± 10	162 ± 10	852 ± 29	147 ± 11	14.9 ± 2.1	4.9 ± 1.2
Top	92 ± 11	77 ± 10	55 ± 7	71 ± 10	4.8 ± 1.4	3.8 ± 1.1
Z/γ^*+ HF	3.2 ± 0.5	70 ± 4	686 ± 33	60 ± 4	7.8 ± 1.4	0.21 ± 0.05
Other	13.1 ± 3.4	14.2 ± 1.9	110 ± 13	15.8 ± 1.2	2.3 ± 0.5	0.9 ± 0.4
HH (×20)	2.70 ± 0.25	1.03 ± 0.22	1.97 ± 0.11	1.22 ± 0.05	5.0 ± 0.6	4.8 ± 0.8
Post-fit Normalisation						
$\mu_{\text{Top}} = 0.79 \pm 0.10$			$\mu_{Z/\gamma^*+\text{HF}} = 1.36 \pm 0.07$			

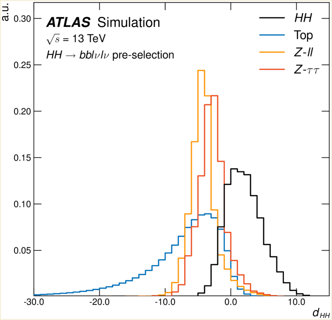

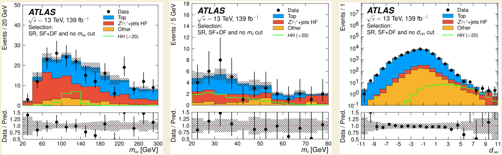

Counting experiment in SRs and CRs → 95% CL upper limits in pb and in units of σ^{HH}_{SM}:

	-2σ	-1σ	Expected	$+1\sigma$	$+2\sigma$	Observed
$\sigma(gg \to HH)$ [pb]	0.5	0.6	0.9	1.3	1.9	1.2
$\sigma(gg \to HH)/\sigma^{\text{SM}}(gg \to HH)$	14	20	29	43	62	40

ATLAS – VBF $HH \to bbbb$

New ATLAS non-resonant HH search result in the VBF channel using almost the full Run-2 dataset (126/fb): ATLAS-CONF-2019-030

The VBF channel has a very small cross-section (1.73 fb at 13 TeV in the SM) but it gives a unique opportunity to probe the c_{2V} coupling.

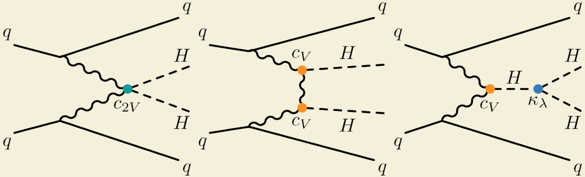

Event selection and analysis strategy:

- New: b-jet energy regression based on a BDT to account for effects beyond the usual calibration;
- VBF jets added to the event selection used in the search for $gg \to HH \to bbbb$:
  - $\geq$2 forward jets with $p_T > 30$ GeV, $|\eta| > 2.0$ and opposite sign of η;
  - $|\Delta\eta_{jj}^{\mathrm{VBF}}| > 5.0$ & $m_{jj}^{\mathrm{VBF}} > 1$ TeV for the 2 highest-p_T forward jets.

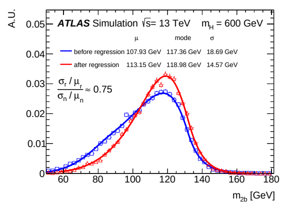

- SR around (123.7 GeV; 116.5 GeV).
- Multi-jet background: weights are derived by comparing $2b + 2j$ and $4b$ samples in a sideband (SB) and applied to a $2b + 2j$ sample of the SR.
- $t\bar{t}$ background: shape from simulation, all-hadronic yield from data, non-all-hadronic yield from the SM prediction.
- ggF $HH \to bbbb$ background: simulation, normalised to the SM prediction.

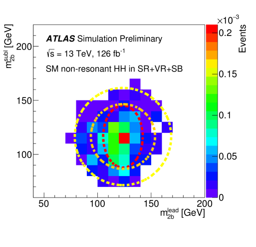

Results:

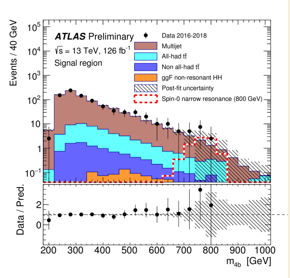

Very first constraint on c_{2V} → observed (expected) between -1.02 (-1.09) and +2.71 (+2.82) at 95% CL.

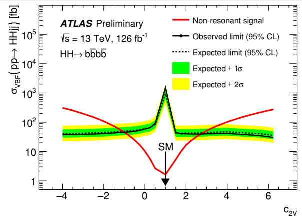

Prospect studies for HH searches at the HL-LHC (and beyond)

ATLAS HH prospects at HL-LHC

$HH \to bbbb$

- Extrapolation of current result to 14 TeV and 3/ab.
- Improved b-tagging efficiency (by 8%).
- Statistical uncertainties are scaled down according to the size of the dataset, while systematic uncertainties remain the same.
- Jet p_T threshold likely to go up because of trigger requirements.

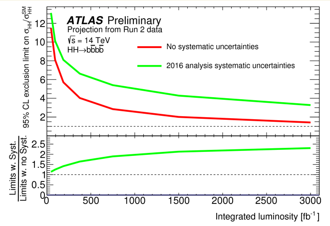

$HH \to bb\tau\tau$

- Extrapolation of current result to 14 TeV and 3/ab.
- Improved b-tagging efficiency (by 8%).
- Re-binning of the BDT + no MC statistical uncertainty + scale down systematic uncertainties of statistical nature and from theoretical modelling.
- Tau p_T threshold likely to go up because of trigger requirements.

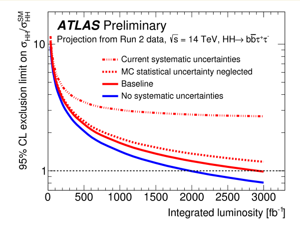

ATLAS HH prospects at HL-LHC

$HH \to bbbb$

- Extrapolation of current result to 14 TeV and 3/ab.
- Improved b-tagging efficiency (by 8%).
- Statistical uncertainties are scaled down according to the size of the dataset, while systematic uncertainties remain the same.
- Jet p_T threshold likely to go up because of trigger requirements.

$HH \to bb\tau\tau$

- Extrapolation of current result to 14 TeV and 3/ab.
- Improved b-tagging efficiency (by 8%).
- Re-binning of the BDT + no MC statistical uncertainty + scale down systematic uncertainties of statistical nature and from theoretical modelling.
- Tau p_T threshold likely to go up because of trigger requirements.

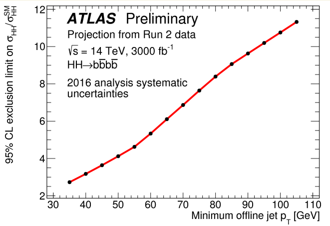

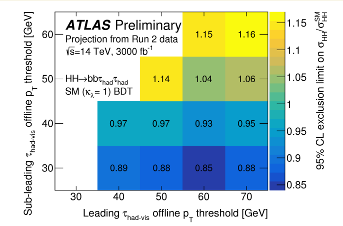

ATLAS HH prospects at HL-LHC

Unlike $HH \to bbbb$ and $HH \to bb\tau\tau$, the prospect study of $HH \to bb\gamma\gamma$ is fully based on simulations at 14 TeV.

- Truth-level particles smeared by detector resolution (μ=200) and weighted according to efficiency or mis-tag rate;
- Two photons ($p_T > 43$, 30 GeV), no isolated leptons and at most five central jets ($p_T > 30$ GeV), of which at least two are b-tagged and have $p_T > 35$ GeV.
- BDT + cut on its score, select $m_{\gamma\gamma} \subset [123; 127]$ GeV, use $m_{bb\gamma\gamma}$ as final discriminant.

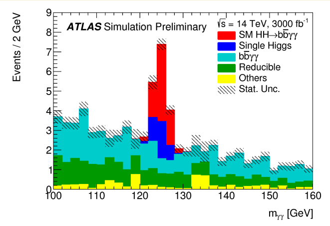

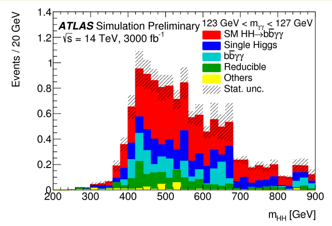

⇒ 95% CL limits at 1.2 (1.1) times σ^{HH}_{SM} with (without) systematic uncertainties.

ATLAS HH prospects at HL-LHC

Statistical combination of $HH \to bbbb$, $HH \to bb\tau\tau$ and $HH \to bb\gamma\gamma$:

- 95% CL limits: 0.68 (0.56) $\times \sigma_{\text{SM}}^{HH}$ with (without) systematic uncertainties.
- Statistical significance of SM HH w.r.t the background-only hypothesis:

Channel	Statistical-only	Statistical + Systematic
$HH \to b\bar{b}b\bar{b}$	1.4	0.61
$HH \to b\bar{b}\tau^+\tau^-$	2.5	2.1
$HH \to b\bar{b}\gamma\gamma$	2.1	2.0
Combined	3.5	3.0

- The relative uncertainty on the signal strength is 40% (31%) with (without) systematic uncertainties.

HH prospects vs κ_λ:

- Constraints on κ_λ from a likelihood ratio test on an Asimov dataset with background + HH with $\kappa_\lambda = 1$;
- Constraints on κ_λ from a likelihood ratio test on an Asimov dataset with background + HH with $\kappa_\lambda = 0$;
- Significance vs κ_λ.

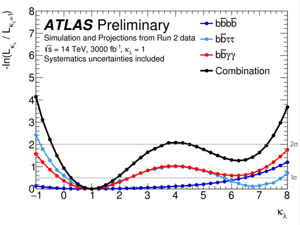

More details in ATL-PHYS-PUB-2018-053

ATLAS HH prospects at HL-LHC

Statistical combination of $HH \to bbbb$, $HH \to bb\tau\tau$ and $HH \to bb\gamma\gamma$:

- 95% CL limits: 0.68 (0.56) $\times \sigma_{\text{SM}}^{HH}$ with (without) systematic uncertainties.
- Statistical significance of SM HH w.r.t the background-only hypothesis:

Channel	Statistical-only	Statistical + Systematic
$HH \to b\bar{b}b\bar{b}$	1.4	0.61
$HH \to b\bar{b}\tau^+\tau^-$	2.5	2.1
$HH \to b\bar{b}\gamma\gamma$	2.1	2.0
Combined	3.5	3.0

- The relative uncertainty on the signal strength is 40% (31%) with (without) systematic uncertainties.

HH prospects vs κ_λ:

- Constraints on κ_λ from a likelihood ratio test on an Asimov dataset with background + HH with $\kappa_\lambda = 1$;
- Constraints on κ_λ from a likelihood ratio test on an Asimov dataset with background + HH with $\kappa_\lambda = 0$;
- Significance vs κ_λ.

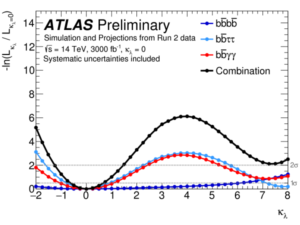

More details in ATL-PHYS-PUB-2018-053

ATLAS HH prospects at HL-LHC

Statistical combination of $HH \to bbbb$, $HH \to bb\tau\tau$ and $HH \to bb\gamma\gamma$:

- 95% CL limits: 0.68 (0.56) $\times\, \sigma_{\text{SM}}^{HH}$ with (without) systematic uncertainties.
- Statistical significance of SM HH w.r.t the background-only hypothesis:

Channel	Statistical-only	Statistical + Systematic
$HH \to b\bar{b}b\bar{b}$	1.4	0.61
$HH \to b\bar{b}\tau^+\tau^-$	2.5	2.1
$HH \to b\bar{b}\gamma\gamma$	2.1	2.0
Combined	3.5	3.0

- The relative uncertainty on the signal strength is 40% (31%) with (without) systematic uncertainties.

HH prospects vs κ_λ:

- Constraints on κ_λ from a likelihood ratio test on an Asimov dataset with background + HH with $\kappa_\lambda = 1$;
- Constraints on κ_λ from a likelihood ratio test on an Asimov dataset with background + HH with $\kappa_\lambda = 0$;
- Significance vs κ_λ.

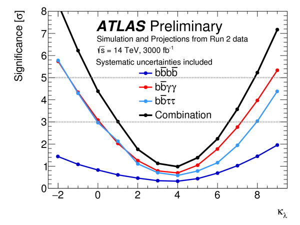

More details in ATL-PHYS-PUB-2018-053

CMS HH prospects at HL-LHC

In contrast with ATLAS, all HH prospect studies use MC simulations of the upgraded CMS detector with DELPHES at 14 TeV, with 200 pile-up events [CMS-PAS-FTR-18-019]:

- $HH \to bbbb$: two $H \to bb$ candidates, mass-dependent selections, either resolved or boosted topologies with a BDT or m_{JJ} as final discriminant. Challenges lie in jet p_T thresholds and multi-jet background estimate.
- $HH \to bb\gamma\gamma$: one BDT against ttH, one BDT against other backgrounds used together with $\tilde{M}_X = m_{\gamma\gamma jj} - (m_{\gamma\gamma} - m_H) - (m_{jj} - m_H)$ to define six event categories, fit of the $m_{\gamma\gamma}$ and m_{jj} distributions.
- $HH \to bb\tau\tau$: three channels ($\tau_e\tau_h$, $\tau_\mu\tau_h$, $\tau_h\tau_h$) each using a DNN output as final discriminant and later combined.
- $HH \to bbVV$: three di-lepton channels, using the shape of a NN to discriminate HH pairs from $t\bar{t}$ and Z/γ^*+jets as final discriminant.
- $HH \to bbZZ$: new decay channel, 4-lepton final state $\Rightarrow$ rare but very clean signature! The main backgrounds are $t\bar{t}$ and Z/γ^*+jets via fake/non-prompt leptons (difficult to estimate).

CMS HH prospects at HL-LHC

Statistical combination:

Extrapolation of the CMS Run-2 results ⇒ significance of 1.8σ with stat. only uncertainties.

Channel	Significance		95% CL limit on $\sigma_{HH}/\sigma_{HH}^{SM}$	
	Stat. + syst.	Stat. only	Stat. + syst.	Stat. only
bbbb	0.95	1.2	2.1	1.6
$bb\tau\tau$	1.4	1.6	1.4	1.3
$bbWW(\ell\nu\ell\nu)$	0.56	0.59	3.5	3.3
$bb\gamma\gamma$	1.8	1.8	1.1	1.1
$bbZZ(\ell\ell\ell\ell)$	0.37	0.37	6.6	6.5
Combination	2.6	2.8	0.77	0.71

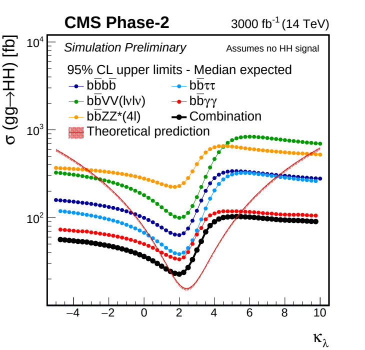

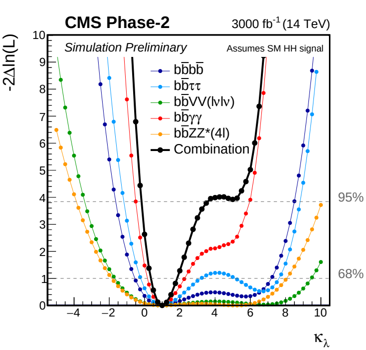

ATLAS+CMS HH prospects at HL-LHC

Combination of ATLAS+CMS HH prospects with no correlations between the different channels, and normalisation to 6/ab for $HH \to bbVV \to bb\ell\ell\nu\nu$ and $HH \to bbZZ \to bb\ell\ell\ell\ell$: see https://arxiv.org/abs/1902.00134

- Combined significance $\gtrsim 4$;
- Minimum negative-log-likelihoods per experiment and channel → the second minimum (degeneracy in event yields) is removed by a low-m_{HH} category in CMS $HH \to bb\gamma\gamma$.

	Statistical-only		Statistical + Systematic	
	ATLAS	CMS	ATLAS	CMS
$HH \to b\bar{b}b\bar{b}$	1.4	1.2	0.61	0.95
$HH \to b\bar{b}\tau\tau$	2.5	1.6	2.1	1.4
$HH \to b\bar{b}\gamma\gamma$	2.1	1.8	2.0	1.8
$HH \to b\bar{b}VV(ll\nu\nu)$	-	0.59	-	0.56
$HH \to b\bar{b}ZZ(4l)$	-	0.37	-	0.37
combined	3.5	2.8	3.0	2.6
	Combined 4.5		Combined 4.0	

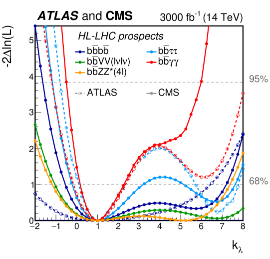

ATLAS+CMS HH prospects at HL-LHC

Combination of ATLAS+CMS HH prospects with no correlations between the different channels, and normalisation to 6/ab for $HH \to bbVV \to bb\ell\ell\nu\nu$ and $HH \to bbZZ \to bb\ell\ell\ell\ell$: see https://arxiv.org/abs/1902.00134

- Combined significance $\gtrsim 4$;
- Minimum negative-log-likelihoods per experiment and channel → the second minimum (degeneracy in event yields) is removed by a low-m_{HH} category in CMS $HH \to bb\gamma\gamma$.
- The 68% confidence interval for κ_λ is [0.52;1.5] with systematic uncertainties.

	Statistical-only ATLAS	Statistical-only CMS	Statistical + Systematic ATLAS	Statistical + Systematic CMS
$HH \to b\bar{b}b\bar{b}$	1.4	1.2	0.61	0.95
$HH \to b\bar{b}\tau\tau$	2.5	1.6	2.1	1.4
$HH \to b\bar{b}\gamma\gamma$	2.1	1.8	2.0	1.8
$HH \to b\bar{b}VV(ll\nu\nu)$	-	0.59	-	0.56
$HH \to b\bar{b}ZZ(4l)$	-	0.37	-	0.37
combined	3.5	2.8	3.0	2.6
	Combined 4.5		Combined 4.0	

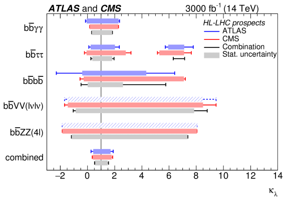

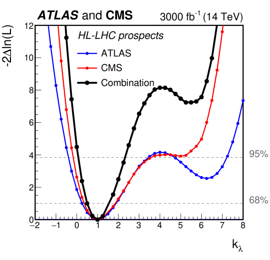

- Exclude second minimum at 99.4% CL.

HH prospects beyond HL-LHC... in one and only one slide

Several of the future colliders on the market will establish the existence of the Higgs self-coupling beyond 5σ and improve the precision on κ_λ (5-10% for CLIC3000 and FCC-hh). Low(er)-energy e^+e^- colliders (below 500 GeV) can only rely on single-H measurements within EFTs to probe κ_λ.

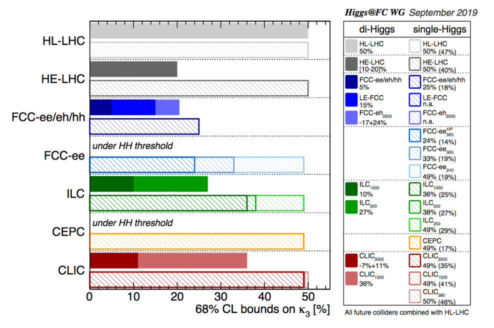

From arxiv:1905.03764

HH prospects prior to HL-LHC?

Talk by E. Vryonidou in the LHCHXSWG-HH meeting of June 17 here.

- **SM EFT:** no light new physics, Higgs SU(2) doublet, addition of dimension-6 operators.
- At leading order, five operators affect Higgs boson pair production, but four of them get constraints from other processes.

$$\mathcal{L}_{\rm Eff} = \mathcal{L}_{\rm SM} + \sum_i \frac{C_i^{(6)} O_i^{(6)}}{\Lambda^2} + \mathcal{O}(\Lambda^{-4})$$

Operator	Constraints
$O_{t\phi} = y_t^3 \left(\phi^\dagger\phi\right)\left(\bar{Q}t\right)\tilde{\phi}\,,$	Inclusive H, Higgs plus jets, ttH
$O_{\phi G} = y_t^2 \left(\phi^\dagger\phi\right) G^A_{\mu\nu} G^{A\mu\nu}\,,$	Inclusive H, Higgs plus jets, ttH
$O_{tG} = y_t g_s (\bar{Q}\sigma^{\mu\nu} T^A t)\tilde{\phi} G^A_{\mu\nu}$	tt, ttH, ttV....
$O_6 = -\lambda(\phi^\dagger\phi)^3$	HH (single Higgs@NLO)
$O_H = \frac{1}{2}(\partial_\mu(\phi^\dagger\phi))^2$	All Higgs couplings H decays, VH, VBF...

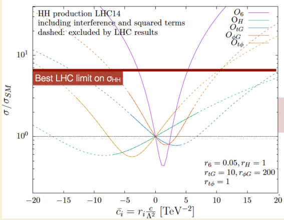

$$O_{t\phi} = y_t^3 \left(\phi^\dagger\phi\right)\left(\bar{Q}t\right)\tilde{\phi}\,,$$

$$O_{\phi G} = y_t^2 \left(\phi^\dagger\phi\right) G^A_{\mu\nu} G^{A\mu\nu}\,,$$

$$O_{tG} = y_t g_s (\bar{Q}\sigma^{\mu\nu} T^A t)\tilde{\phi} G^A_{\mu\nu}$$

$$O_6 = -\lambda(\phi^\dagger\phi)^3$$

$$O_H = \frac{1}{2}(\partial_\mu(\phi^\dagger\phi))^2$$

Currently, the Higgs boson self-coupling κ_λ can still be constrained by ignoring the other EFT couplings.

HH prospects prior to HL-LHC?

Talk by E. Vryonidou in the LHCHXSWG-HH meeting of June 17 here.

- **SM EFT:** no light new physics, Higgs SU(2) doublet, addition of dimension-6 operators.
- At leading order, five operators affect Higgs boson pair production, but four of them get constraints from other processes.

$$\mathcal{L}_{\rm Eff} = \mathcal{L}_{\rm SM} + \sum_i \frac{C_i^{(6)} O_i^{(6)}}{\Lambda^2} + \mathcal{O}(\Lambda^{-4})$$

Operator	Constraints
$O_{t\phi} = y_t^3 \left(\phi^\dagger \phi\right)\left(\bar{Q} t\right)\tilde{\phi}\,,$	Inclusive H, Higgs plus jets, ttH
$O_{\phi G} = y_t^2 \left(\phi^\dagger \phi\right) G^A_{\mu\nu} G^{A\mu\nu}\,,$	Inclusive H, Higgs plus jets, ttH
$O_{tG} = y_t g_s (\bar{Q}\sigma^{\mu\nu} T^A t)\tilde{\phi} G^A_{\mu\nu}$	tt, ttH, ttV….
$O_6 = -\lambda(\phi^\dagger\phi)^3$	HH (single Higgs@NLO)
$O_H = \frac{1}{2}(\partial_\mu(\phi^\dagger\phi))^2$	All Higgs couplings H decays, VH, VBF…

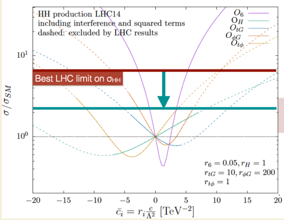

$O_{t\phi} = y_t^3 \left(\phi^\dagger \phi\right)\left(\bar{Q} t\right)\tilde{\phi}\,,$

$O_{\phi G} = y_t^2 \left(\phi^\dagger \phi\right) G^A_{\mu\nu} G^{A\mu\nu}\,,$

$O_{tG} = y_t g_s (\bar{Q}\sigma^{\mu\nu} T^A t)\tilde{\phi} G^A_{\mu\nu}$

$O_6 = -\lambda(\phi^\dagger\phi)^3$

$O_H = \frac{1}{2}(\partial_\mu(\phi^\dagger\phi))^2$

In the (close?) future, a global fit with information from differential distributions will be needed. Strategy?

EFT couplings were varied one by one here.

A simultaneous fit may change the picture!

Summary

- ATLAS and CMS have recently published many HH search results with a partial Run-2 dataset at 13 TeV:
  - ATLAS: best 95% CL upper limit by ATLAS at 6.9 times the SM prediction + κ_λ constrained between -5 and +12 at 95% CL;
  - ATLAS: first single- and double-Higgs-boson combination;
  - CMS: 95% CL limits set in various EFT-inspired scenarios (shape benchmarks).
- Very new results in ggF $HH \to bb\ell\ell\nu\nu$ and VBF $HH \to bbbb$ using the full Run-2 dataset!
- Prospect studies: the HL-HLC should exclude the absence of Higgs self-coupling at more than 95% CL and reach a 50% precision on κ_λ.
- Until then, HH searches in ATLAS and CMS should focus more and more on interpretations within EFTs (including results from single-H measurements).

HH is one of the most exciting (and challenging) field to work with in high-energy physics... now and for many years to come!

Back-up slides

Resonant HH searches

ATLAS – resonant HH – combination

- Spin-0 heavy scalar: all final states, NLO signal model except in $bbbb$ and $bb\tau\tau$.
- Spin-2 KK graviton: only $bbbb$, $bb\tau\tau$ and $bbWW$, LO signal model, here with $k/\overline{M}_{\mathrm{Pl}} = 1 \Rightarrow 95\%$ exclusion for 310–1380 GeV.

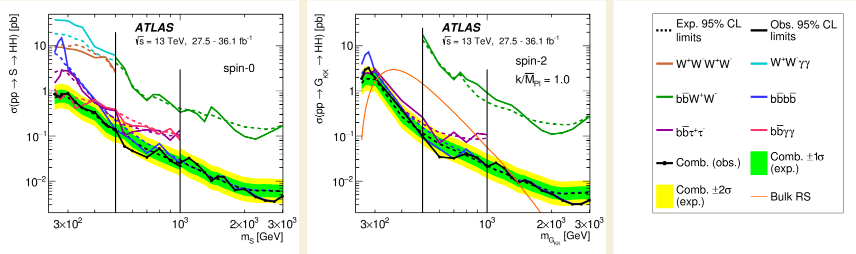

https://arxiv.org/abs/1906.02025

ATLAS – resonant HH – combination

- Spin-0 heavy scalar: all final states, NLO signal model except in $bbbb$ and $bb\tau\tau$.
- Spin-0 interpretations: exclusion limits in the EWK-singlet model (left) and hMSSM (right), using $bbbb$+$bb\gamma\gamma$+$bb\tau\tau$.

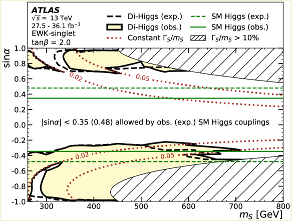

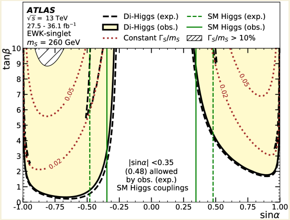

Exclusion limits are shown only when the resonance width remains smaller than the experimental resolution.

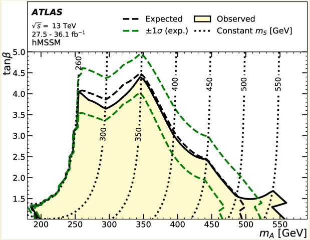

https://arxiv.org/abs/1906.02025

CMS – resonant HH – combination

- CP-even particle of spin-0 (radion) or spin-2 (graviton) with a width much smaller than the detector resolution for the whole mass range.

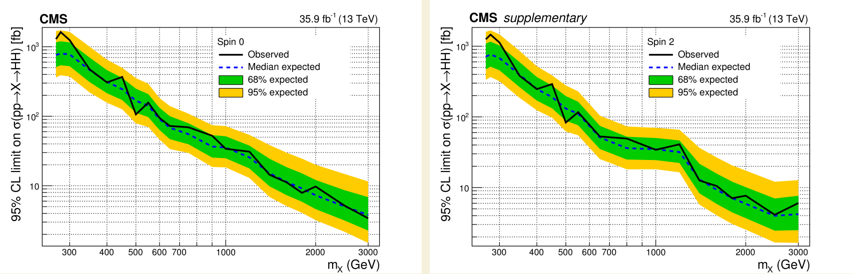

Phys. Rev. Lett. 122 (2019) 121803